

FIRST QUARTERLY REPORT:
SOLAR CELL PERFORMANCE
MATHEMATICAL MODEL

CASE FILE COPY

Prepared for the
California Institute of Technology
Jet Propulsion Laboratory

By M.J. Barrett

Exotech Incorporated
525 School Street, S.W
Washington, D.C. 20024

September 15, 1969

FIRST QUARTERLY REPORT:
SOLAR CELL PERFORMANCE
MATHEMATICAL MODEL

Prepared for the
California Institute of Technology
Jet Propulsion Laboratory

By M. J. Barrett

Exotech Incorporated
525 School Street, S.W.
Washington, D.C. 20024

September 15, 1969

This work was performed for the Jet Propulsion Laboratory,
California Institute of Technology, as sponsored by the
National Aeronautics and Space Administration under
Contract NAS7-100.

This report contains information prepared by Exotech Incorporated under JPL subcontract. Its content is not necessarily endorsed by the Jet Propulsion Laboratory, California Institute of Technology, or the National Aeronautics and Space Administration.

TABLE OF CONTENTS

Section	Page
INTRODUCTION.	1.
I. SUMMARY OF SOLAR CELL PERFORMANCE	2.
II. ANALYSIS OF MATHEMATICAL MODEL.	5.
A. Comparison With Recent Literature	5.
B. Computation Techniques	9.
C. Electron Shielding Calculations	13.
III. PROTON DAMAGE STUDIES	18.
A. Depth Dependence of K	18.
B. Model Predictions	19.
IV. STATUS OF COMPUTER PROGRAM.	25.
V. CONCLUSIONS	26.
A. General Summary	26.
B. Future Work	26.
C. New Technology.	27.
REFERENCES.	28.

TABLE OF CONTENTS

Section	Page
INTRODUCTION.	1.
I. SUMMARY OF SOLAR CELL PERFORMANCE	2.
II. ANALYSIS OF MATHEMATICAL MODEL.	5.
A. Comparison With Recent Literature	5.
B. Computation Techniques	9.
C. Electron Shielding Calculations	13.
III. PROTON DAMAGE STUDIES	18.
A. Depth Dependence of K	18.
B. Model Predictions	19.
IV. STATUS OF COMPUTER PROGRAM.	25.
V. CONCLUSIONS	26.
A. General Summary	26.
B. Future Work	26.
C. New Technology.	27.
REFERENCES.	28.

INTRODUCTION

This is the first quarterly report on a one year program to provide computational methods for prediction of solar cell performance in a natural radiation environment. It covers work performed during the period 1 June 1969, through 31 August 1969. A model, permitting theoretical calculations for solar cell performance under such a mixed-radiation environment, was previously prepared under contract 952246 with the Jet Propulsion Laboratory, Pasadena, California. That model, reported by Exotech on February 28, 1969, is the basis for the effort reported herein. The successful adaptation of such a model in a computerized version sensitive to environmental parameters is clearly an invaluable aid in design, selection, and performance predictions for individual spacecraft power systems.

For readers unfamiliar with the previous work, Section I provides a brief synopsis and review of the mathematical terminology introduced. Section II and III are really the substance of this report; they contain the progress achieved in the past three months. It will be obvious, on reading these sections, that portions of the model have been adapted to a computer to permit the investigations reported. To indicate the extent of this adaptation, Section IV presents the current status of the program. Finally, conclusions regarding this work and observations of potentially fruitful areas for photovoltaic research are presented as Section V.

I. SUMMARY OF SOLAR CELL PERFORMANCE

The photovoltaic effect at a silicon diode junction was discovered as early as 1941, ⁽¹⁾ but practical silicon solar cells were not available until 1954. These solar cells converted sunlight with an efficiency around 6% and opened up the possibility of rugged, long-lived, light power sources for special applications. An interesting review of early developments of the solar cell is given by Crossley, Noel, and Wolf. ⁽²⁾

Modern solar cells for spacecraft applications are typified by Figure 1. The cell area may be from 1 x 2 cm to 3 x 3 cm, with a cell thickness of 8-12 mils (dimensions are conventionally given in these heterogeneous units). A junction is formed about 0.5 micron (5×10^{-5} cm) below the sunward surface; this junction separates the thin "surface" region of n-type silicon from the thicker "base" region of p-type silicon. For the sunward side, the electrical contact is in the form of a bar along one edge and a number of thin grid lines extending from it across the surface. The dark side contact generally completely masks the back surface of the cell.

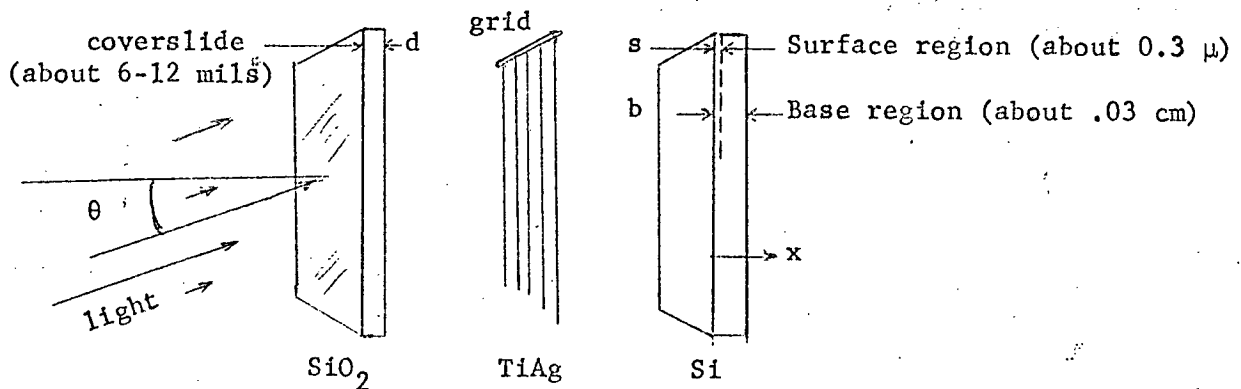


Figure 1. Exploded view of typical solar cell, with notation as used in text.

Illumination of this device results in the sunward surface being a fraction of a volt positive with respect to the back surface. A current is thereby induced in an electrical connection between the front bar and the back contact. This is not equal, however, to the current generated by the sun (photovoltaic current), for some of the photovoltaic current is returned through the solar cell itself, in accordance with its diode property. This leads to the solar cell equation, which principally states that the electrical current flowing from a solar cell equals the difference between the photovoltaic current I_L produced in it, and the diode current I_D lost in it.

The output of the solar cell depends on a large number of independent factors. First, the intensity of sunlight and the angle of incidence are important. A cell directly facing the sun receives the maximum possible sunlight. If it deviates from this direction by an angle θ , as shown in Figure 1, the radiant energy striking the cell is reduced by the cosine of θ . As the angle increases, edge effects, especially when a coverslide is used, make the reduction deviate slightly from this law, and measurement must be relied on for each specific geometry when extreme accuracy is required for solar cells illuminated at large angles from the perpendicular.

The output of solar cells has frequently been characterized by the short-circuit current I_{sc} , the open circuit voltage V_{oc} , and the power and voltage of the cell near its maximum power point. While these parameters do characterize the electrical output, in the present work more basic terms are used. These are the photovoltaic current I_L , the diode parameters I_0 and V_0 , and the internal series resistance R . These four parameters are chosen since it is a more straight-forward exercise to determine from semiconductor theory how they are affected by the environment and history of a solar cell. Nevertheless, both set of parameters are related, and knowing one set permits a calculation of the other.

In this connection, it is helpful to note that I_{sc} nearly equals I_L , that R is generally less than 0.5 ohms, and that V_0 is on

the order of 40 millivolts. An example of numerical values in the solar cell equation is presented in section II.

Aside from the obvious factor of illumination, the other factors affecting solar cell performance include its temperature T and the fluence of atomic particles Φ to which it has been exposed.

The fluence of natural radiation in the space environment is composed of many species of atomic particles, but only protons and electrons need to be considered for their damaging effects. To determine the effects of this radiation on solar cells, it is necessary to (a) evaluate the proton and electron fluences as functions $\Phi_p(E)$ and $\Phi_e(E)$ of energy, (b) evaluate and sum the damage due to these fluences that occurs in the solar cell material, (c) evaluate the changes in the solar cell electrical characteristics as functions of this damage.

The current I at a voltage V across the solar cell may be evaluated from its radiation history, as described above, and a knowledge of its construction, as indicated by Figure 1, the illumination, and the temperature. This is the task of our mathematical model.

II. ANALYSIS OF MATHEMATICAL MODEL

A. Comparison with Recent Literature

A continuing search of the current literature is being undertaken in order to determine the existence of possible variations to the mathematical model we have adopted ⁽³⁾ for solar cell performance. This search indicates that validity of the diode equation for silicon solar cell applications is being tested by several investigators.

The current-voltage characteristic of the solar cell is assumed to be equivalent to that of a current source, shunted by a diode, and with a series resistance. The equation resulting from this assumption is the conventional "solar cell equation." We have developed curve-fitting techniques that so far have shown this equation to fit experimental curves with a high accuracy under all conditions of illumination and radiation degradation. Similar success has been reported by Brown. ⁽⁴⁾ To demonstrate the accuracy possible with the simple solar cell equation even for unconventional cell types, we present two curve fits in Figure 2 to lithium-doped solar cells. Generally, our curve fits have been almost, but not quite, this good.

Theoretically, the solar cell equation appears to be a good first approximation. This is borne out by its accuracy in fitting current-voltage (IV) measurements. However, deviations of measurements from the equation have been reported. Wolf and Rauschenbach ⁽⁶⁾ have recommended that the current source be assumed to be shunted by two diodes with different characteristic voltages. The revised solar cell equation, in our notation, would then take the form

$$I = I_L - I_{o1} \left[e^{\frac{(V+IR_{s1})}{V_{o1}}} - 1 \right] - I_{o2} \left[e^{\frac{(V+IR_{s2})}{V_{o2}}} - 1 \right] \quad (1)$$

This has the immediate advantage of allowing two extra parameters for curve fitting, and the disadvantage of relating these parameters to the individual solar cell and its environment. The rationale for the extra diode term must be developed if it is to be adopted in a general mathematical model.

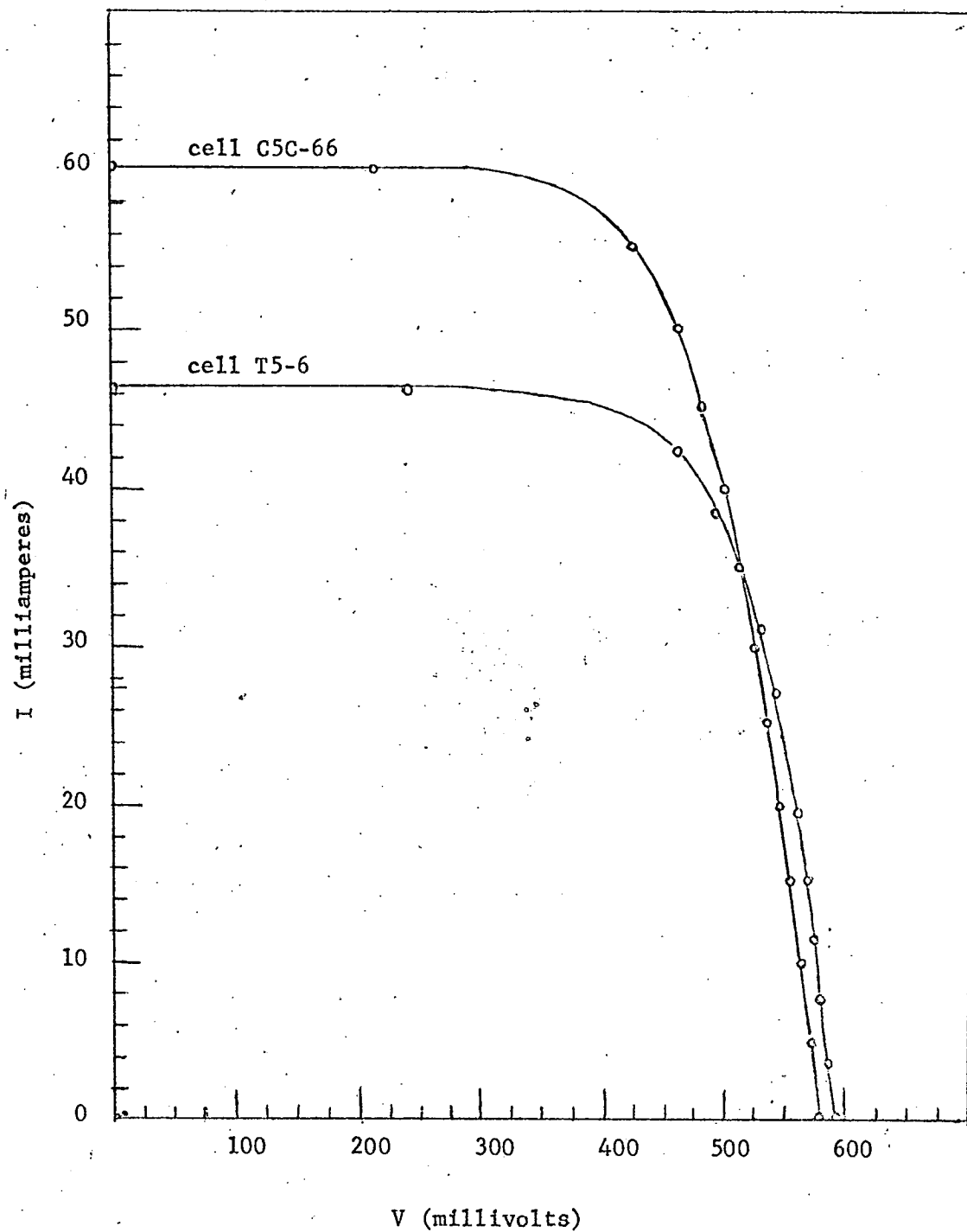


Figure 2. Comparison of measured IV curves for lithium cells⁽⁵⁾
with points computed with the solar cell equation:

$$I = 60.2 - 1.675 \times 10^{-4} (e^{(V+.791I)/45.34} - 1) \quad \text{top curve}$$

$$I = 46.3 - 1.625 \times 10^{-4} (e^{(V+.322I)/46.98} - 1) \quad \text{bottom curve}$$

Schoffer and Beckman (7), studying the response of solar cells to intense illumination, derived this model from theory. Much of the series resistance R_s in the cell is due to the sheet resistance of the surface layer, through which the current must flow from all points of the junction area to reach to grid lines. With large currents, this results in a appreciable voltage gradient on the junction area, with IR drops in voltage between points at the grid lines and points far from them. Thus, a distributed diode potential exists, and the two-diode model of Wolf and Rauschenbach can be considered as an approximation to the distribution. Further, measurements of open circuit voltage as a function of illumination plot as a slightly curved line in a semilog plot; instead of a straight line as predicted by the simple solar cell equation. This is interpreted as indication that, with a change in the IR drop along the surface, the voltage across the diode changes, and the relative magnitudes of the two diode currents shift.

This last point is worthy of a more detailed discussion. Consider a solar cell with negligible resistance R_s , which obeys the simple solar cell equation. Then I_L equals I_{sc} , and

$$I = I_{sc} - I_o (e^{V/V_o} - 1) \quad (2)$$

This rearranges to

$$I_{sc} - I = I_o (e^{V/V_o} - 1) \quad (3)$$

Since V_o is typically about 50 millivolts, when the voltage V is greater than 350 millivolts, e^{V/V_o} is greater than 1096 and, to better than 99.97% accuracy,

$$I_{sc} - I = I_o e^{V/V_o} \quad (4)$$

For such a solar cell. This means that a plot of the logarithm of $(I_{sc} - I)$ versus the voltage V , beyond the knee of the I-V curve which generally occurs around 350 mv, should be a straight line

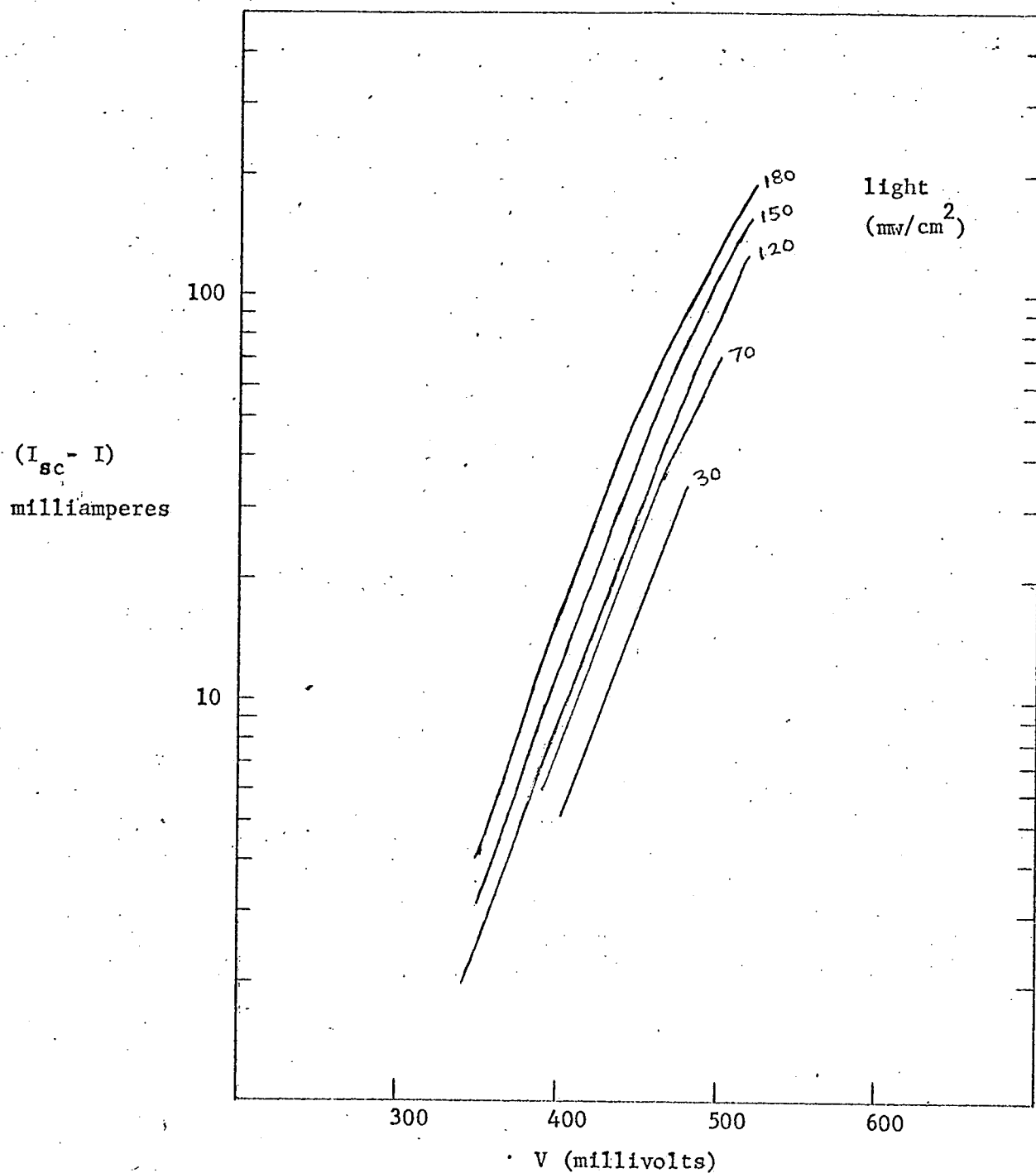


Figure 3. A plot of the diode current ($I_{sc} - I$) from data taken with different light intensities.⁽⁸⁾ The plots are straight where the data obey a simple, resistance-less solar cell equation. Resistance would make the lines concave upward. The observed downward concavity suggest the existence of additional diode effects.

with slope determined by V_0 and extrapolated intercept determined by I_0 .

An attempt at such a result is shown in Figure 3. The lines, drawn for different illumination intensities, are almost straight, but not quite. It appears that when the diode current ($I_{sc} - I$) is less than about 40 mv, the lines are parallel and straight. This has the effect of making some solar cells deviate from simple diode theory when the illumination is great, as was discussed.

Whatever the reason, this indicates that the simple solar cell equation is only an approximation. The model is inaccurate when the diode current is large; 40 ma in a 2 cm^2 cell appears to be the borderline.

It is not necessary to invoke distributed diodes to derive a curvature such as exhibited in Figure 3. Ladany⁽⁹⁾ has presented an analysis of a one-dimensional diode, such as the solar cell, which results in a forward characteristic reminiscent of that shown in Figure 3. His analysis leads to an expression, however, that does not require additional parameters to duplicate the characteristic.

B. Computation Techniques

The heart of the Exotech mathematical model is a difference solution for the continuity equation. This allows a calculation of the minority carrier profile across the cell for arbitrary light spectrum and for nonuniform damage by radiation.

The difference technique employs a mesh interval h whose width determines the convergence of the solution. It appears reasonable to assume that the smaller h is near the junction, the better-defined is the profile there. Since the minority carrier distribution near the junction determines the photovoltaic current, it is desirable to calculate it as precisely as possible. To demonstrate this convergence, we present Figure 4 from earlier work. The figure suggests that decreasing the mesh interval improves accuracy, to a point where h is about a quarter of a micron. Whether there is an optimum mesh interval, as suggested by the figure, must be determined by more detailed comparisons.

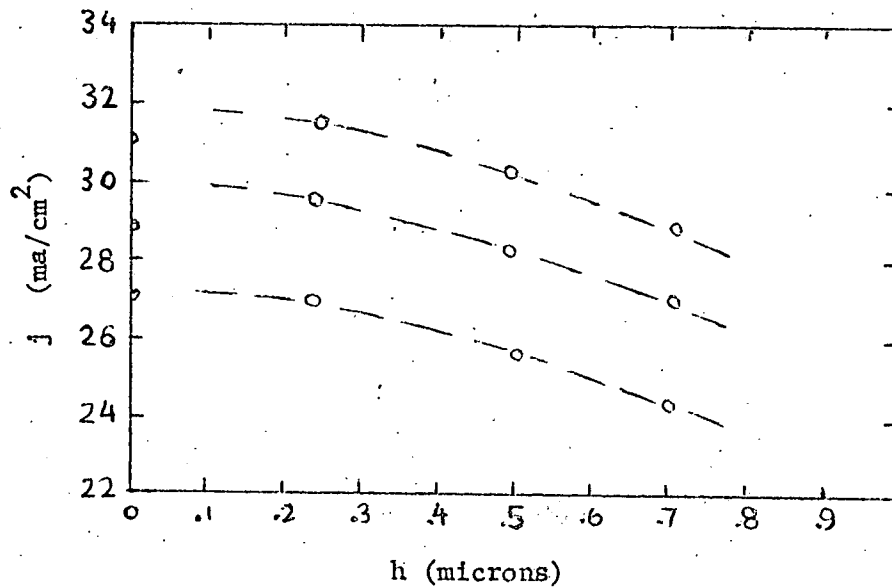


Figure 4. Calculated values of short-circuit current density versus mesh interval h , for three cells with different base minority carrier diffusion lengths L .

Small mesh intervals such as these are undesirable in terms of computer time to solve the continuity equation. If h is uniformly 0.25 microns, crossing the base region of a typical 10 mil cell would require about 1000 intervals. Each iteration of the calculation would have that many steps.

However, such precision is not necessary near the back of the solar cell. The ideal scheme for small mesh size near the junction, yet reasonably rapid computer time, would therefore be use of a formula by which a mesh interval h_k increases with distance x_k from the junction. We selected the formula

$$h_k = k\Delta \quad (5)$$

If, then, the distance b is to be divided into n intervals, the first interval will have a width

$$\Delta = 2b/n (n + 1) \quad (6)$$

and the last or nth interval will have width $n\Delta$. As an example, with only 50 intervals in a 10 mil distance, the first has a width 0.2 microns.

To utilize this scheme, it is necessary to rederive the difference equation for a mesh of variable width h_k . The first and second derivatives of the minority carrier concentration, designated n_k at the beginning of the kth interval, must be evaluated. The approximate derivation we used is based on Figure 5.

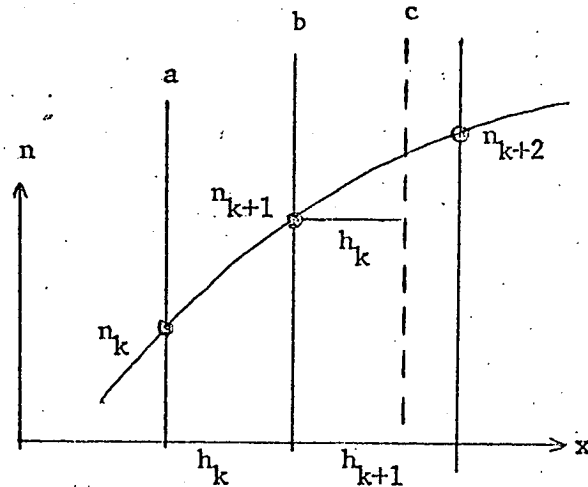


Figure 5. Construction of variable mesh h_k to approximate the curve $n(x)$ at points n_k

Figure 5. Construction of variable mesh h_k to approximate the curve $n(x)$ at points n_k .

Approximating the curve $n(x)$ by straight line segments joining points n_k and using the definitions of the derivative in calculus, we have

$$\left(\frac{\Delta n}{\Delta x} \right)_b = \left[n_{k+1} + \left(\frac{h_k}{h_{k+1}} \right) (n_{k+2} - n_{k+1}) - n_k \right] / 2h_k \quad (7)$$

where b denotes where the first derivative is computed: this is at n_{k+1} .

Precise calculation of the second derivative at n_{k+1} requires more points than the three in the figure. This leads to difficulties in the continuity equation. However, it can be recalled that h_k is generally small, so that the first derivative changes little within each interval. From n_k to n_{k+1} in the figure, the first derivative is approximately

$$\left(\frac{\Delta n}{\Delta x} \right)_a = \frac{n_{k+1} - n_k}{h_k} \quad (8)$$

and from n_{k+1} to n_{k+2} the first derivative is approximately

$$\left(\frac{\Delta n}{\Delta x} \right)_c = \frac{n_{k+2} - n_{k+1}}{h_{k+1}} \quad (9)$$

So that the second derivative at n_{k+1} is approximately

$$\left(\frac{\Delta^2 n}{\Delta x^2} \right)_b = \frac{h_k n_{k+2} - (h_k + h_{k+1}) n_{k+1} + h_{k+1} n_k}{2h_k^2 h_{k+1}} \quad (10)$$

These expressions for the first and second derivatives transform the continuity equation into a difference equation, with variable mesh size. After some routine shuffling, the terms can be organized to yield

$$\begin{aligned} n_{k+2} \left[h_k + h_k^2 qE/kT \right] &= n_{k+1} \left[h_k (1 + h_k qE/kT) + h_{k+1} (1 - h_k qE/kT) \right] \\ - n_k \left[h_{k+1} (1 - h_k qE/kT) - 2h_k^2 / L_k^2 \right] & \\ - \left[2h_k^2 h_{k+1} G_{k+1} / D \right] & \end{aligned} \quad (11)$$

This replaces the earlier formulation of the difference equation to permit faster, more accurate calculation.

C. Electron Shielding Calculation

An elaborate curve fit was presented in the mathematical model to relate the spectrum of electrons in the natural environment with the spectrum striking a solar cell that is covered by a fused silica coverglass. This fit has been programmed in the last quarter and accurate calculation of the transmitted spectrum was found to require an undesirably long and detailed calculation.

The difficulty is in the shape of the spectrum formed when monoenergetic electrons are slowed down in a coverglass. A typical spectrum, as seen in Figure 6, includes most of the transmitted electrons in an almost monoenergetic peak. This peak decreases, and the transmitted spectrum becomes flatter as the coverglass thickness approaches the range of the incident electrons.

We found that the curve fit to the spectrum can not be integrated by ordinary analytic techniques. This forced us to program the computer to calculate points on the curve, and generate damage integrals by a piecewise approximation

$$\langle K_e \Phi \rangle_k = \sum_{E_1} K_e(E_1) \Phi_e(E_1, x_k) \quad (12)$$

where $K_e(E_1)$ is the electron damage coefficient for transmitted energy E_1 and $\Phi_e(E_1, x_k)$ is the flux, evaluated from the curve fitted spectrum, of energy E_1 due to monoenergetic electrons of energy E_0 slowing down through a shield of thickness x_k . (The notation here is unchanged from the previous report.)

Strictly speaking, $\Phi_e(E_1, x_k)$ should be a piecewise integration, covering all of the spectrum in an energy interval about E_1 .

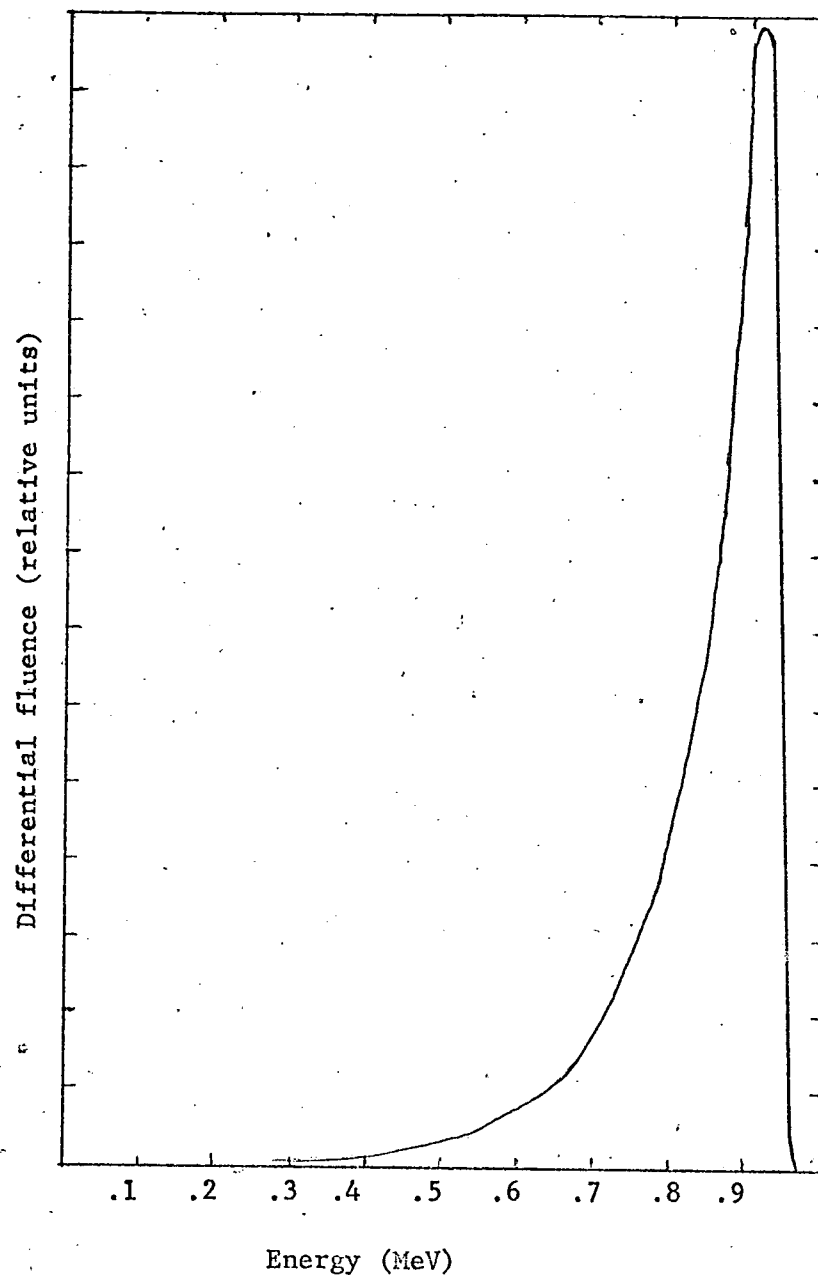


Figure 6. The calculated spectrum of electrons which have penetrated 0.055 gm/cm^2 of aluminum, due to 1 MeV electrons incident isotropically over a hemisphere. (10)

If the spectrum were reasonably flat, this could be approximated by calculating the energy-differential flux at energy E_1 and multiplying it by the width of the interval. The peak in the spectrum makes this an impractical approach.

Our most recent programming has followed an idea previously presented.⁽¹¹⁾ The redefined formula is

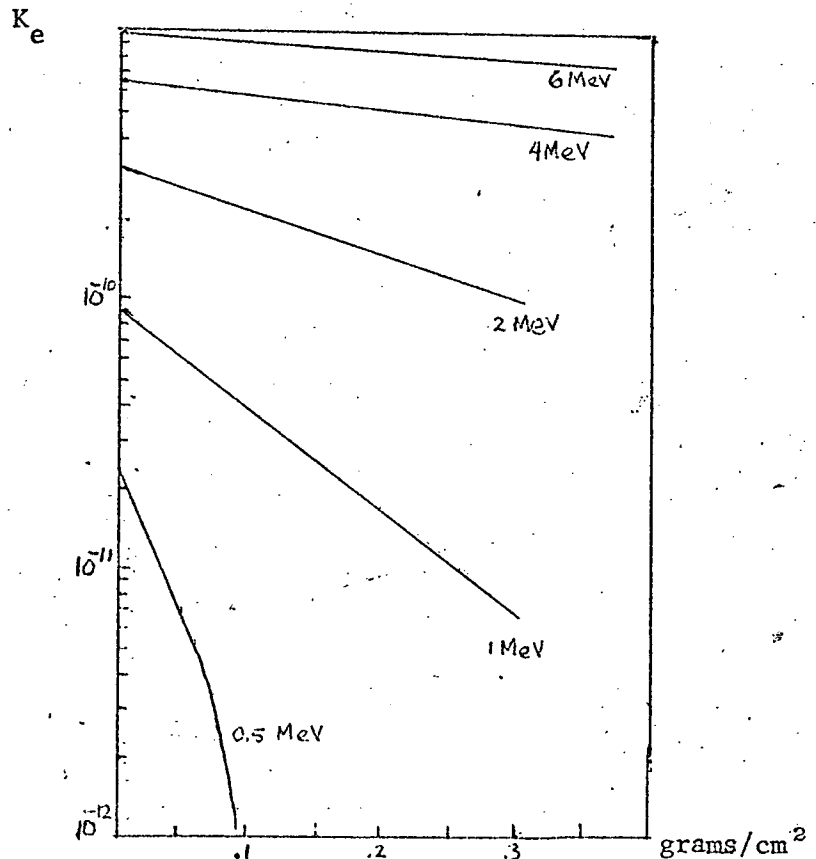
$$\langle K_e \Phi \rangle_k = \sum_{E_1} K_e(E_1, x_k) \Phi_e(E_1) \quad (13)$$

where E_1 is now an energy of the incident, or natural environment, electron spectrum and the electron damage coefficients are modified by the shield thickness x_k .

When the solar cell is covered with ρd grams/cm² of coverslide, the electron flux due to incident monoenergetic electrons of energy E is given by a spectrum, of energies less than E , dependent on the thickness ρd of shielding. This spectrum can then be weighted by the damage coefficient as a function of energy to obtain an effective damage coefficient $K_e(E, \rho d)$ for the shielded solar cell with electrons of energy E incident on the shield.

Several results of this calculation are shown in Figure 7, where

Figure 7. Effective damage coefficient of electrons as a function of coverslide thickness (gms/cm²) and incident energy



the damage coefficient, per unit incident particle, appears to decrease exponentially ($e^{-\mu_{pd}}$). When pd approaches the electron range, of course, the proportion rapidly drops to zero. Further, the fitting parameter μ appears to have a simple dependence on energy. The slopes of the curves are plotted, in Figure 8, versus incident particle energy.

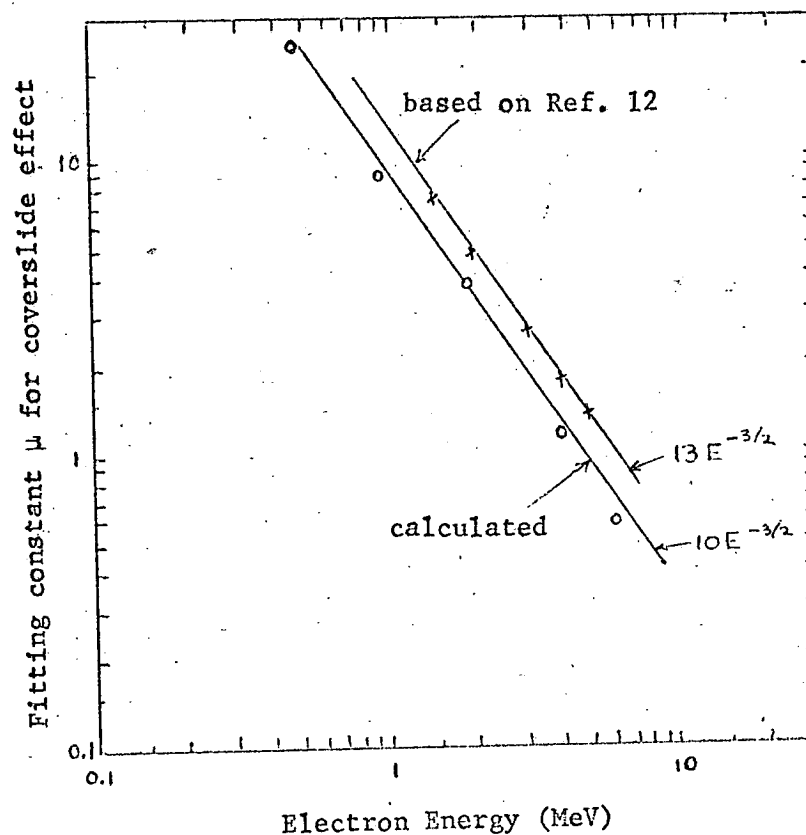


Figure 8. Plot of negative slopes of straight lines in Figure 7 versus electron energy, compared with negative slopes that would yield data of Ref.12 for solar cells shielded with a 0.3 gm/cm^2 coverslide (See Eq. 4)

The results fit well to an analytical expression:

$$K_e(E, pd) = K(E, 0) \exp(-10pd/E^{1.5}) \quad (14)$$

where pd is the coverslide areal density, in gm/cm^2 . The equation 14 is obviously adaptable to the problem of determining the necessary coverslide thickness for solar cells on a given mission. K is now the effective damage coefficient, having been reduced in magnitude by the presence of the coverslide.

We have compared our results with the early experimental work of Brown et al (12). Using a beam at different angles on bare and variously-covered cells, they constructed the damage curves for n/p solar cells for electron energies up to 3 MeV, and extrapolated to 7 MeV. Assuming that the damage is given by the data for bare cells and the data for cells covered with 0.3 gm/cm^2 coverslides, and by a simple exponential $\exp(-\mu pd)$ at other thicknesses, we have computed μ as a function of energy. The energy dependence of the function μ is also shown in Figure 8. The dependence on E again indicates a minus 1.5 power law; the magnitude of μ is however, about 30% greater. Part of this discrepancy may be due to the decrease in ionization loss by electrons with higher atomic weight of the shield.

III. PROTON DAMAGE STUDIES

A. Depth Dependence of K

Because a proton slows down as it travels to a stop in a medium, its damage effectiveness increases. The result is that K may be considered as a function of depth x into a solar cell such that the change in diffusion length L varies with depth. The angular distribution about the normal to the surface describing the incident proton flux affects this distribution. As an example of the magnitude of the variation with depth, consider the case where the incident flux is isotropic and the variation of K with energy E is simple K_0/E where K_0 is the damage coefficient for 1 MeV protons.

Let μ equal the cosine of angle θ of incidence, as shown in Figure 9. The energy of a proton in its travel can be determined from the range $R_0 E_0^n$ of the proton. By integration over all possible

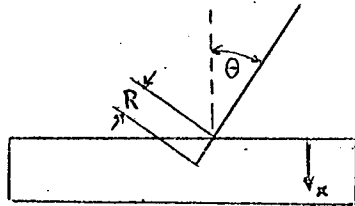


Figure 9. Proton stopping in solar cell

angles of incidence, the expression for K is obtained.

$$K(x) = 2\pi \int_{\mu_0}^1 \frac{1}{4\pi} \left[\frac{K_0}{E_0^n - \frac{x}{R_0 \mu}} \right] \frac{1}{n} d\mu \quad (15)$$

where μ_0 is the cosine of the maximum angle of incidence through which a proton of energy E_0 can penetrate to the depth x.

The expression 2π represents integration over the azimuthal angle, and the incident proton flux is normalized to $(1/4\pi)$ protons per steradian. With the substitution

$$z = E_0^n - \frac{x}{R_0 \mu} \quad (16)$$

the integral is transformed to

$$K(x) = \frac{K_0(x)}{2R_0} \int_0^{(E_0^n - x/R_0)} \frac{dz}{z^{1/n} [E_0^n - z]^2} \quad (17)$$

Even with the simplifications presented so far, this integral is formidable. With n equal to about 1.75, $1/n$ equals 0.57. As an approximation, let $1/n$ equal 0.5. Then a closed form solution is obtained:

$$K(x) = \frac{K_0}{2 E_0} \left[\left(1 - \frac{x}{R}\right)^{\frac{1}{2}} + \frac{x}{R} \ln \frac{1 + \left(1 - \frac{x}{R}\right)^{\frac{1}{2}}}{1 - \left(1 - \frac{x}{R}\right)^{\frac{1}{2}}} \right] \quad (18)$$

where R is the initial range of the protons.

The various parts of the expression may be interpreted. The expression K_0/E_0 represents the damage coefficient of the incident protons. The factor $1/2$ represents the shielding of the back hemisphere by the cell. The expression in brackets represents both the reduction in number of the protons with depth x and the increasing damage of the remaining protons as their energy drops. This expression is plotted in Figure 10. It can be seen that the drop in energy at first enhances the damage, but the drop in number eventually takes over and reduces the damage until it vanishes at the point where depth x equals proton range R . This is quite different from the damage profile of monoenergetic protons entering the solar cell in a parallel beam. The damage is "smeared" for the isotropic incidence; it is "peaked", as suggested by the familiar Bragg curve, for the parallel beam.

B. Model Predictions

A major outstanding problem in the prediction of radiation effects to solar cells is the calculation of damage from protons that do not completely penetrate the crystal. The model developed under Contract 952246 provided an original method for calculation of the effects of nonuniform damage in solar cells, such as generated by low energy protons. Thus, these proton damage relationships could be evaluated for the first time in depth. Previous work has been based on "equivalence" or "effective" measured parameters.

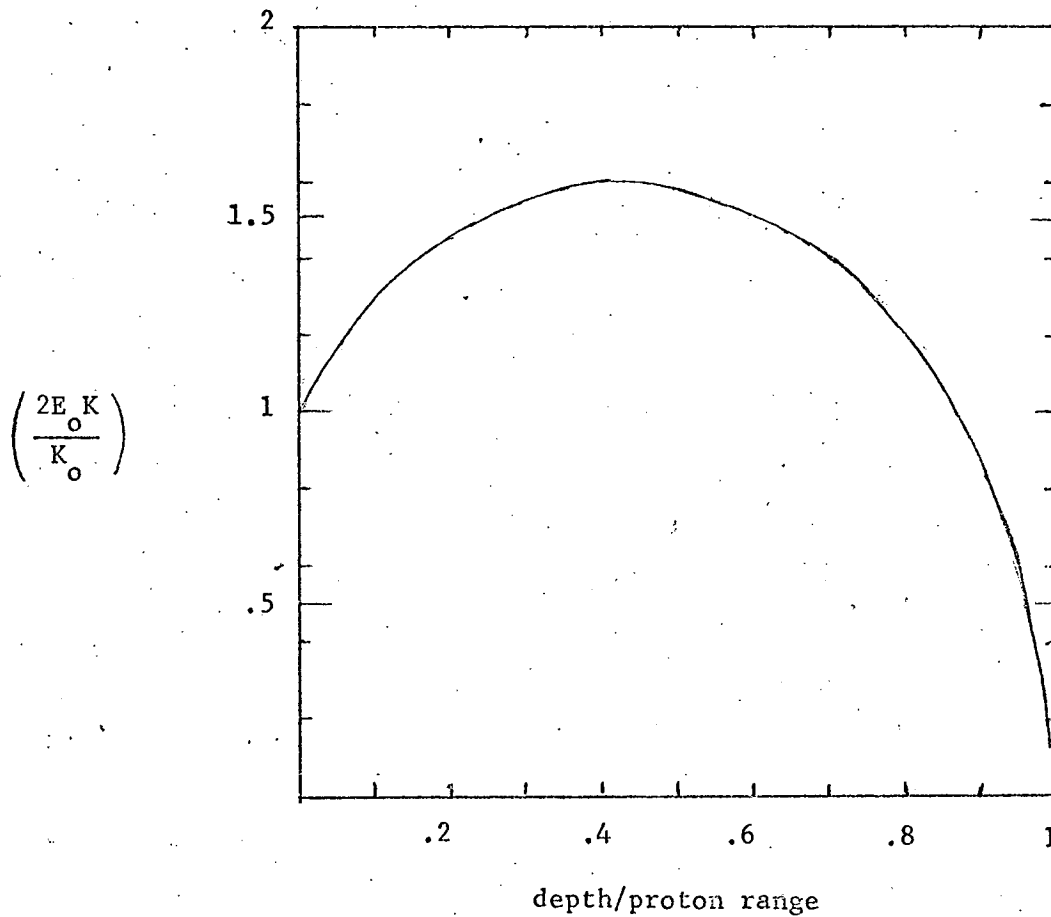


Figure 11. The damage due to unit isotropic fluence, normalized to the surface damage due to a unit parallel-beam fluence of protons. Plotted as a function of depth of penetration into the solar cell, with the depth normalized to the proton range (Approximate, from Eq. 18)

As a first possibility, it might be possible that our value of the damage coefficient is too high. The measurement of proton damage coefficients is obviously difficult, in view of the rapid change of proton energy even in a small silicon crystal. Further, the coefficient will depend on crystal resistivity, type of dopant, and even temperature during bombardment. These dependences are poorly understood and no simple formulas exist to represent them. Thus, K could easily have been overestimated. If, for example, it were a factor of 3 lower than assumed, then the model would estimate a given decrease in I_L after one-third of the proton fluence actually required.

It is a simple matter to check such a possibility. Figure 11 includes a dashed line for the calculation where K is reduced, for all proton energies, by a factor of 3. The alternate model generated in this way approaches the measurement, but some further scaling of K will show that a reasonably accurate fit is not possible from simple scaling.

A second possibility that might be considered here is interference between defects at the end of the track of the proton. Each proton produces about 5×10^5 displacements/cm as it is slowed down from an energy of 10 keV to 1 keV. Conceivably, in a large fluence of protons, many of the collisions that occur could be with silicon atoms that have already been displaced. These can not be counted as additional defects and therefore should not add to the damage. However, under the assumption that all silicon atoms, whether displaced or in lattice positions, are equally likely to be struck by a proton, we calculate that this interference should be significant when the proton fluence is of the order of $10^{17}/\text{cm}^2$.

As was shown in the last section, the proton damage coefficient can be computed as a function of depth into the solar cell. The generalization of this calculation to the proton spectrum in space is obvious. When a coverslide is present, the parameter x in Eq. 17 must be measured from the front surface of the coverslide. Taking these considerations into account in the model, we compute the damage, and hence the values L_K of the minority carrier coefficient as a function of depth in the cell. Eq. 11 can then be solved for the minority carrier concentration, and hence the current. In theory, this precise analysis is preferable over the practice of estimating an effective damage coefficient and an effective L for the cell.

With this detailed analysis, we still find in some cases that theory overestimates the reduction in current. The experiment compared with is an extreme one: monoenergetic protons were directed perpendicular to a solar cell. Thus, the damage is strongly peaked near the end of the range of the protons, and L_K has a strong discontinuity. The depth in the cell at which this occurs is about 3.3 microns. The results we have obtained are shown in Figure 11. Several possibilities exist to explain why low energy protons are not damaging as predicted.

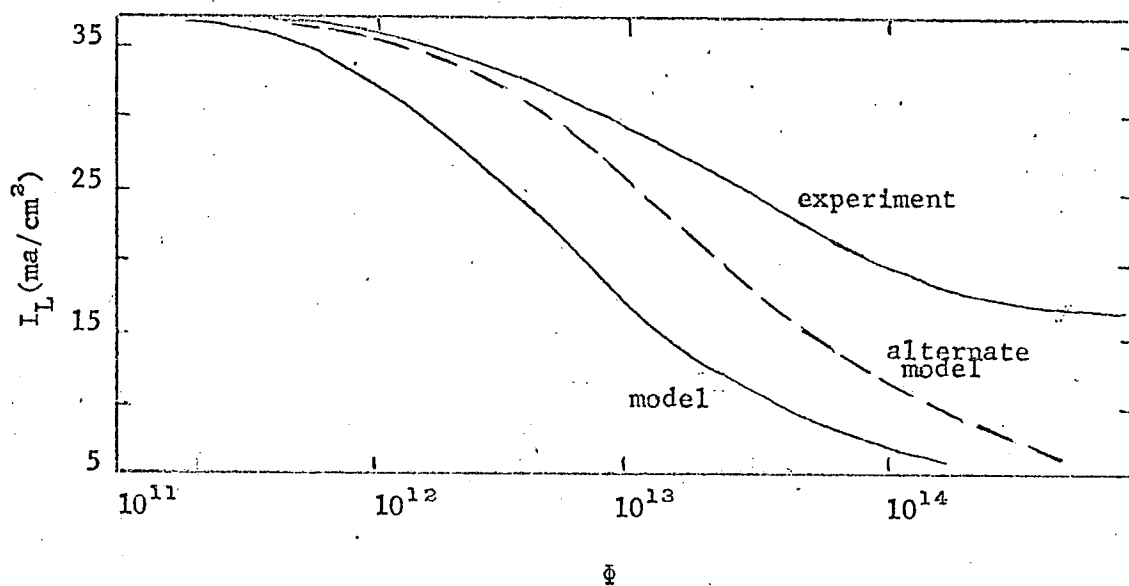


Figure 11. Photovoltaic current versus 270 keV proton fluence. The dashed line is based on the assumption that the damage coefficient used is a factor of 3 too large.

The deviation between theory and measurement occurs much lower, around fluences of the order $10^{12}/\text{cm}^2$. However, the assumption made may be in error; the displaced silicon atoms could be more likely to be struck than are the lattice atoms. This would be a channeling effect, whereby lattice atoms, particularly those at the end of the proton track, shadow each other to reduce a collision probability. This needs a more detailed theoretical investigation.

Another possibility is that displacements occur and interfere with each other. A lattice vacancy, according to theory, diffuses through the lattice until it finds a stable configuration. One such configuration is a recombination center, which is electrically active in reducing the carrier density. Another configuration, of course, would be a vacancy filled with a silicon that had been interstitial. This would be electrically inactive, and be readily evaluated in terms of theory.

A fourth possibility for investigation takes into account the proton, or hydrogen ion, that is left at the end of the track. The proton could combine either with a nearby vacancy or with a recombination center to reduce its damage effectiveness. This would be local form of annealing, perhaps similar to that noted with lithium. (These atoms are similar, having the same valence, and similar size.)

Finally, the recombination center may persist but be incorrectly evaluated. The current study does not include evaluation of fill factors, which are known to be significantly affected by illumination intensity. This topic has recently been of concern and is the subject of current investigations elsewhere. Fill factor for proton-induced recombination centers is a function of light intensity, and therefore can vary through the cell. This is because light is strongly attenuated in silicon. The light intensity at the recombination center is therefore a function of its distance from the surface of the cell.

The majority of these possible explanations invoke some sort of interference between defects. If one of these is correct, a laboratory experiment with monoenergetic protons in a parallel beam should create less damage than the same fluence in space. As shown in the previous

section, the assumption of an isotropic space fluence leads to a damage constant K that varies smoothly through the cell, and there is no region of dense damage. This would decrease the amount of defect interference, displacement interference, or localized annealing. As a result, damage would be distributed more evenly through the solar cell and possibly more accurately predicted by theory.

An experiment that would shed light on the true nature of proton damage could be readily performed in the laboratory. This would consist of measurements of proton damage to solar cells that initially were matched as to crystal orientation, junction depth, efficiency, etc. A proton energy, in the neighborhood of 1 MeV, would be selected, and each cell would be bombarded at a different angle with respect to the beam, with a fluence on the order of $10^{13}/\text{cm}^2$. The current output of the damaged cells would then be measured under a solar simulator. The results would provide a test of common assumptions that the damage resides at the origin of the defect, that channeling is of no concern, etc. A careful comparison of the results with the model should permit a better understanding of the effects of non-uniform damage and the diffusion of charges in silicon.

IV. STATUS OF COMPUTER PROGRAM

Portions of the mathematical model have been programmed and run with test data on the IBM 360. These runs have led to the several modifications for the model that are discussed earlier in this report. Thus, the computer program at present exists as a series of routines subject to revision of theory and technique. Future effort is necessary to compact and join these routines.

The central routine developed so far is the calculation of the photovoltaic current, via an analysis of the continuity equation. The variable mesh size h_k which is discussed in section IIB is now incorporated in this program. The operator enters the program in the machine, together with data on cell thickness, junction depth, etc. The program can calculate minority carrier concentration on both sides of the junction and sum the photovoltaic currents from both sides.

Three routines have been written to determine the damage integrals due to trapped protons, trapped electrons, and flare protons. In the first two of these, a fine mesh has been set for the spectrum so that reasonable accuracy appears possible when the spectrum is assumed flat in the interval. For flare protons, a spectrum varying as E^{-x} is assumed and the portion of the damage integral due to the high energy tail is performed analytically.

Finally, a short routine has been written to compute the source term G_k for minority carriers due to the absorption of light. Values of the light absorption coefficient of silicon are stored in this routine. The spectrum of space sunlight is also stored; a future option that would be useful would be to include other useful spectra such as tungsten arc, etc. The routine presently does not include consideration of reflection losses.

V. CONCLUSIONS

A. General Summary

Results of the first three months of an effort to prepare a computer program for solar cell performance in space are reported. Improvements of a mathematical nature have been noted: the application of a variable mesh interval in the difference equation, and the re-grouping of factors in the electron shielding calculation to avoid a rapidly-varying function.

Analytically, an investigation into the diode property of the solar cell has been conducted. This has lead to an upper bound in diode current, beyond which a more detailed model is necessary.

Problems encountered are discussed. These are principally with regard to the nonuniform damage by protons. An approximate analysis of the damage due to monoenergetic protons, incident isotropically, is presented. Arguments are developed from this analysis to indicate that the discrepancy between model results and laboratory experiments should be greater than between model results and performance in space.

The computer program, existing as a series of independent routines, is in the process of formulation into a single package.

B. Future Work

Future work will include further analysis of solar cell performance in light of current theory and observation, preparation of the completed computer program, debugging and checkout, and evaluation of the program.

The analysis of solar cell performance at present is concentrated on the problem of nonuniform damage. It should be noted that only when the fluence reaches the rather high value of 10^{12} does the model deviate appreciably from experimental data and, furthermore, reasons exist to indicate this deviation may be smaller for space fluences than for laboratory fluences. Further effort on this problem should permit calculation of damage with higher values of proton fluence.

The completed computer program shall be capable of predicting the power degradation of solar cells in a combined environment of low and high energy protons and electrons and provide the necessary framework to optimize the solar cell coverglass combination for a particular radiation environment with respect to cell base resistivity, cell thickness, coverslide thickness, and cell substrate type and thickness. The program is to be presented in operable form, listed in Fortran IV, suitable for input to an IBM 360-50.

Standard modular debugging will be employed for program checkout. It will be tested and evaluated against published experimental results and continually updated throughout the course of this contract as additional experimental data is analyzed.

C. New Technology

After a diligent review of the work performed under this contract, it was determined that no new innovation, discovery, improvement or invention was developed.

REFERENCES

1. Scaff, J.H., Theuerer, H.C., and Schumacher, E.E.
Trans. AIME 185, 383 (1949)
2. Crossley, P.A., Noel, G.T., and Wolf, M., "Review and Evaluation of past Solar-Cell Development Efforts" RCA Report AED R-3346. June 1968.
3. Barrett, M.J., and Stroud, R.H., "A Model For Silicon Solar Cell Performance in Space," Final Exotech Report on JPL contr. 952246. February 1969.
4. Brown, W.D., Hodgman, G.W., and Spreen, A.T., "Computer Simulation of Solar Array Performance," Sixth Photovoltaic Conf. March 1967.
5. Downing, R.G., Carter, J.R., Scott, R.E., and Van Atta, W.K.
"Study of Radiation Effects in Lithium Doped Silicon Solar Cells"
Final TRW Report on JPL Contr. 952251. May 1969.
6. Wolf, M., and Rauschenbach, H, "Series Resistance Effects on Solar Cell Measurements," Advanced Energy Conversion Vol. 3, pp 455-479. 1963.
7. Schoffer, P., and Bechman, W.A., "Evaluation of A Distributed Model of a Photovoltaic Cell", Sixth Photovoltaic Conf. March 1967.
8. Ritchie, D.W., and Sandstrom, J.D., "Multi-Kilowatt Solar Arrays," Sixth Photovoltaic Conf. March 1967.
9. Ladany, I., "DC Characteristics of a Junction Diode," Proceedings of the IRE. April 1959.
10. Lopez, M., of MSFC, Houston (private communication).
11. Barrett, M. J., "Electron Damage Coefficients in P-type Silicon", IEEE Trans. on Nuc. Sci. NS-14, No.6 December 1967.